Fermilab Library
0 1160 0011020 9
MAD-PH-717
SEP 1 1992

University of Wisconsin–Madison

MAD/PH/717
August 1992

# SUPERCOLLIDER PHYSICS*

V. Barger
*Physics Department, University of Wisconsin, Madison, WI 53706, USA*

ABSTRACT

A smorgasbord is set out of important Standard Model (SM) and Beyond the Standard Model physics possibilities that can be explored for the first time at the SSC, LHC, LEP II and future $e^+e^-$ supercolliders. The areas considered are multiple top- and $W$-boson production, jet-tagging techniques to detect the SM heavy Higgs boson in the channel $H \to WW \to$ leptons, the detectability of the minimal supersymmetric SM Higgs boson at planned machines and the design requirements for the next linear $e^+e^-$ collider so that a no-lose search can be made for the MSSM Higgs bosons.

## Introduction

The much higher collision energies to be reached at $pp$ and $e^+e^-$ supercolliders now under construction or design will make possible the study of many important physics possibilities for the first time. This report singles out four interesting new areas of study that touch on the most pressing issues in post-modern particle physics, namely the nature of electroweak symmetry breaking and the existence of supersymmetry.

In the context of the Standard Model (SM) the SSC and LHC hadron machines will have the capability of exploring the physics associated with production of multiple $W$-bosons and top quarks. A Higgs boson with mass $m_H > 2M_W$ produced in association with $t\bar{t}$ leads to $4W$ events as does $t\bar{t}t\bar{t}$ production. Such SM multiple-$W$ sources are surveyed in § 1 and their relevance to Beyond the Standard Model (BSM) physics of supersymmetry is explored. The pair production and cascade decays of gluinos lead to multiple $W$-boson final states. Fortunately, the gluino signal exceeds the $t\bar{t}t\bar{t}$ background for gluino masses of order 1 TeV.

The search for a heavy SM Higgs boson in the $H \to WW \to$ leptons channel can be accomplished at the SSC/LHC provided that an energetic quark jet from $qq \to qqWW$ is tagged, thereby suppressing the SM QCD background. High $p_T$ jets in the central region must also be vetoed in order to reject the background from $t\bar{t}$ production. The success of this technique, described in § 2, has also been extended to $ZZ$ and $WZ$ final states.

Invited talk at the *Beyond the Standard Model III Conference*, Carleton University, June 1992.

The detectability of the Higgs bosons of the Minimal Supersymmetric Standard Model (MSSM) is considered in § 3 following a brief review of their masses and couplings, including the radiative corrections due to a heavy top quark. A systematic discussion is presented of the MSSM parameter space coverage that will be possible at LEP II and the SSC. (Coverage at the LHC is comparable to that of the SSC provided that the LHC luminosity is a factor of 10 higher.) A small inaccessible window of parameters remains at present.

The existence of this window of inaccessibility for discovery of MSSM higgs bosons at hadron colliders leads naturally to the question of what are the minimal energy and luminosity requirements for an $e^+e^-$ machine that could make a "no-lose" search. The answer to this question, given in § 4, depends on the top quark mass because the radiative corrections to the lightest CP-even Higgs boson depends strongly on $m_t$. For $m_t = 150\,\mathrm{GeV}$ and a 1 TeV supersymmetry scale, full coverage of the MSSM parameter space is achieved at $\sqrt{s} = 215\,\mathrm{GeV}$ with $\mathcal{L} = 20\,\mathrm{fb}^{-1}$ or at $\sqrt{s} = 230\,\mathrm{GeV}$ with $\mathcal{L} = 10\,\mathrm{fb}^{-1}$. This result is relevant to design considerations for the next linear $e^+e^-$ collider.

## 1. Multiple $W$ and Multiple Top Quark Production

Present machines explore the varied and interesting physics associated with multi-leptons. In the future, hadron supercolliders will probe the even richer physics associated with multi-weak boson production[1] and thereby make precision tests of the Standard Model gauge theory couplings and hopefully also discover new physics Beyond the Standard Model (BSM). The first calculations focussed on direct production of $W$-bosons via lowest order subprocesses. Subsequent studies evaluated the contributions of the $2 \to 2$ subprocesses[2]

$$q\bar{q} \to \begin{cases} W^+W^-\,, & W^\pm\gamma \\ W^\pm Z\,, & Z\gamma \\ ZZ \end{cases} \tag{1}$$

and their bearing on tests[3] of the non-Abelian gauge structure of the theory at $p\bar{p}$ and $pp$ colliders. Other $2 \to 2$ processes[4]

$$gg \to \begin{cases} W^+W^- \\ ZZ \end{cases} \tag{2}$$

proceed through quark loop diagrams and constitute a significant addition to the background to the signal of a heavy Higgs boson[5,6] with kinematically allowed $H \to W^+W^-, ZZ$ decays. The tree-level production of three weak bosons[7]

$$q\bar{q} \to \begin{cases} W^+W^-W^+ \\ W^+W^-Z \\ W^\pm ZZ \\ ZZZ \end{cases} \tag{3}$$

was found to have a strong dependence on the Higgs boson mass, with large enhancements in the cross section when $m_H > 2M_W$. The direct production of four weak bosons has also been calculated for the two channels[8]

$$q\bar{q} \to \begin{cases} W^+W^-W^+W^- \\ ZZZZ \end{cases} \tag{4}$$

expected to give the largest and smallest cross section, respectively, for such final states.

Although the preceding channels are extremely interesting, the production of top quarks will lead to much larger cross sections for multi-$W$ events, since the branching fraction for $t \to Wb$ decay is $\simeq 100\%$ for $m_t > M_W + m_b$ (except in non-standard models with a charged Higgs boson where $t \to H^+b$ may be competitive). Recently the SM cross sections have been determined for the following final states with top quarks[9]

$$gg, q\bar{q} \to \begin{cases} t\bar{t}t\bar{t} \\ t\bar{t}W^+W^- \\ t\bar{t}ZZ \end{cases} \tag{5}$$

Some new calculational technology is required.[9,10] For example, the process $gg \to t\bar{t}t\bar{t}$ has 72 Feynman diagrams and a $76 \times 76$ color matrix (a diagram with a 4-gluon coupling contributes 3 distinct color structures). Numerical methods were employed[9] in calculating the amplitudes at the Dirac spinor level and in doing the color sums and diagonalizing the color factor matrix. Similar methods were used in calculating the cross sections of other subprocesses.[1]

Some multiple-$W$ cross sections expected at the SSC (with CM energy $\sqrt{s} = 40\,\text{TeV}$) are listed below,[1,9] taking $m_t = 140\,\text{GeV}$ and $m_H = 400\,\text{GeV}$.

| parent process | $\sigma$ (fb) | multi-$W$ state |
|---|---|---|
| $t\bar{t}$ | $10^7$ | $2W$ |
| $t\bar{t}b\bar{b}$ | $10^5$ | $2W$ |
| $WW$ | $10^5$ | $2W$ |
| $t\bar{t}Z$ | $10^4$ | $2W1Z$ |
| $t\bar{t}W$ | $2 \times 10^3$ | $3W$ |
| $3W$ | $5 \times 10^2$ | $3W$ |
| $t\bar{t}t\bar{t}$ | $4.0 \times 10^2$ | $4W$ |
| $t\bar{t}H$ | $3.4 \times 10^2$ | $4W$ |
| $t\bar{t}WW$ | $1.7 \times 10^2$ | $4W$ |
| $4W$ | 6 | $4W$ |

(6)

The corresponding numbers of events may be estimated by multiplying by an annual SSC luminosity of $\mathcal{L} = 10\,\text{fb}^{-1}$. Jet multiplicity, vertex detection, and $W$ or $Z$ isolation may be used to separate the sources. These various multi-$W$ processes are of intrinsic interest in the SM and are potential backgrounds to BSM physics.

We note that the production of multiple $b$-quarks should be measurable at the Tevatron with vertex detectors.[1] With $p_T > 15\,\text{GeV}$ for each detected $b$-quark, an

assumed $b$-detector efficiency of 0.3 and Tevatron luminosity $100\,\mathrm{pb}^{-1}$, there would be 400 events with 3 $b$'s detected (200 events with 4 $b$'s detected).

An example of BSM physics with multi-$W$ events is the production of the gluino pairs of supersymmetry.[1,11] The gluinos decay copiously to top quarks

$$\tilde{g} \to t\bar{t}\tilde{Z}_i\,, \qquad \tilde{g} \to tb\tilde{W}_i^{\pm}\,. \tag{7}$$

These decays are enhanced by the large top Yukawa couplings.[11] For a gluino of 1 TeV mass, the approximate branching fractions to multiple real $W$ boson final states, based on cascade decay calculations with the program SUSYBF,[11] are[8]

| decay | branching fraction |
|---|---|
| $\tilde{g} \to W$ | 30% |
| $\to WW$ | 30% |
| $\to WWZ$ | 6% |
| $\to 4W$ | 6% |

(8)

The resulting $\tilde{g}\tilde{g} \to nW$ signals potentially have backgrounds from SM $4t$ production. Fortunately the $4W$ signal exceeds the background for a substantial range of gluino mass in the example shown in Fig. 1 where only real $W$-boson contributions are included.

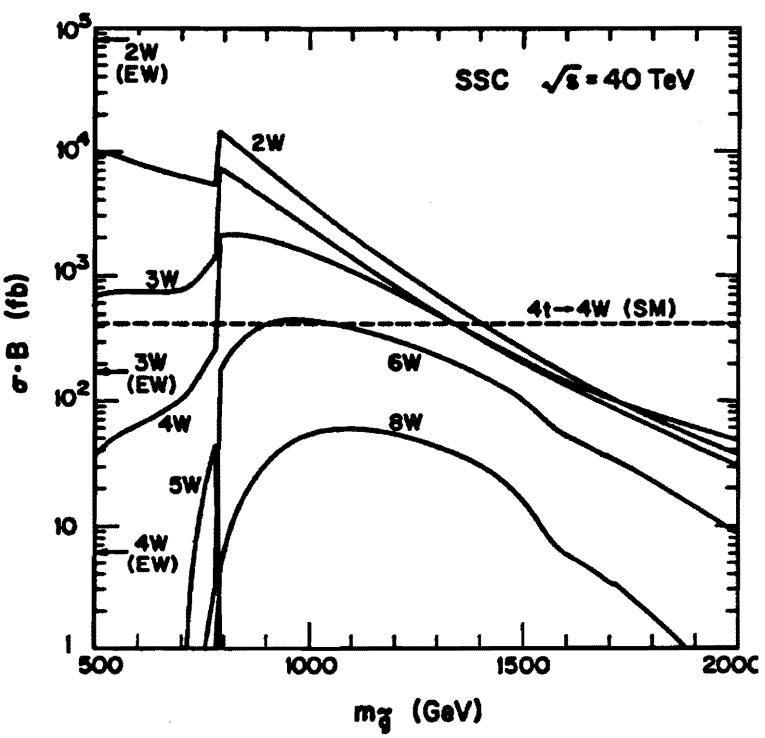


Fig. 1. Cross sections times branching fractions for producing various numbers of real $W$ bosons from $\tilde{g}$ pair production and subsequent $\tilde{g}$ decays at the SSC. The dashed horizontal line indicates the cross sections for $pp \to 4t \to 4W$ production. From Ref. 9.

## 2. Single Forward Jet-Tagging to Search for a Heavy SM Higgs boson

In the search for the source of electroweak symmetry breaking, we must be prepared to detect a SM Higgs boson at the SSC/LHC over the entire mass range

$$\text{LEP II bound} \lesssim m_H \lesssim 1\,\text{TeV}\,, \tag{9}$$

where the expected reach of LEP II is about $M_W$. Even if a heavy Higgs boson is non-existent, there may well be similar effects of electroweak symmetry breaking origin in the $WW$ and $ZZ$ sectors.[12] Therefore we need to be able to isolate the weak boson scattering subprocesses $qq \to qqWW(ZZ)$, illustrated in Fig. 2. Two methods have been proposed to accomplish this:

(i) Forward jet tagging[6,13–18] with a central jet veto,[6,16]

(ii) Large rapidity gap signatures[18–20]

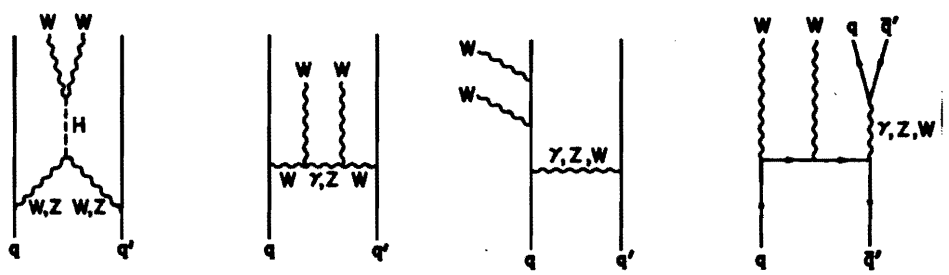


Fig. 2. Representative diagrams for the electroweak processes $qq \to qqW^+W^-$.

In the case that both weak bosons decay leptonically, the two methods are very similar in spirit. In the present discussion, the prospects for identifying the $qq \to qq$"$H$" process by tagging forward jets and rejecting central jet activity, will be assessed. First attempts at forward jet tagging imposed high energy requirements, $E_j \sim 1\,\text{TeV}$, on both forward jets, but such double tagging suppresses the signal too severely. In successful recent applications[6,16,17] only a single jet tag is imposed.

The backgrounds to be overcome are illustrated in Fig. 3. For single jet tagging the $\mathcal{O}(\alpha_s)$ QCD diagrams for gluon or quark exchange must be considered. There are also electroweak backgrounds, such as photon exchange, that give transversely polarized $W$ or $Z$ bosons. However, the dominant and most difficult to eliminate $WW$ background is due to top quark pair production and $t \to bW$ decays. Here an extra radiated gluon is the most likely to produce the hard forward tag jet, rather than the $b$-quarks from top decays. The electroweak backgrounds from the weak boson fusion subprocesses are estimated using a light Higgs boson ($m_H = 100\,\text{GeV}$) calculation.

In order to avoid the severe QCD $Wjj$ backgrounds that may mask the $WW$ signal, leptonic decays of both $W$-bosons are considered.[16] This search channel has a sizeable signal $B(H \to W^+W^- \to \ell\bar{\nu}\bar{\ell}\nu) \simeq 3\%$ in comparison to the leptonic modes for $ZZ$ final states of $B(H \to ZZ \to 4\ell) \simeq 0.14\%$ and $B(H \to ZZ \to \ell\bar{\ell}, \nu\bar{\nu}) \simeq 0.8\%$.

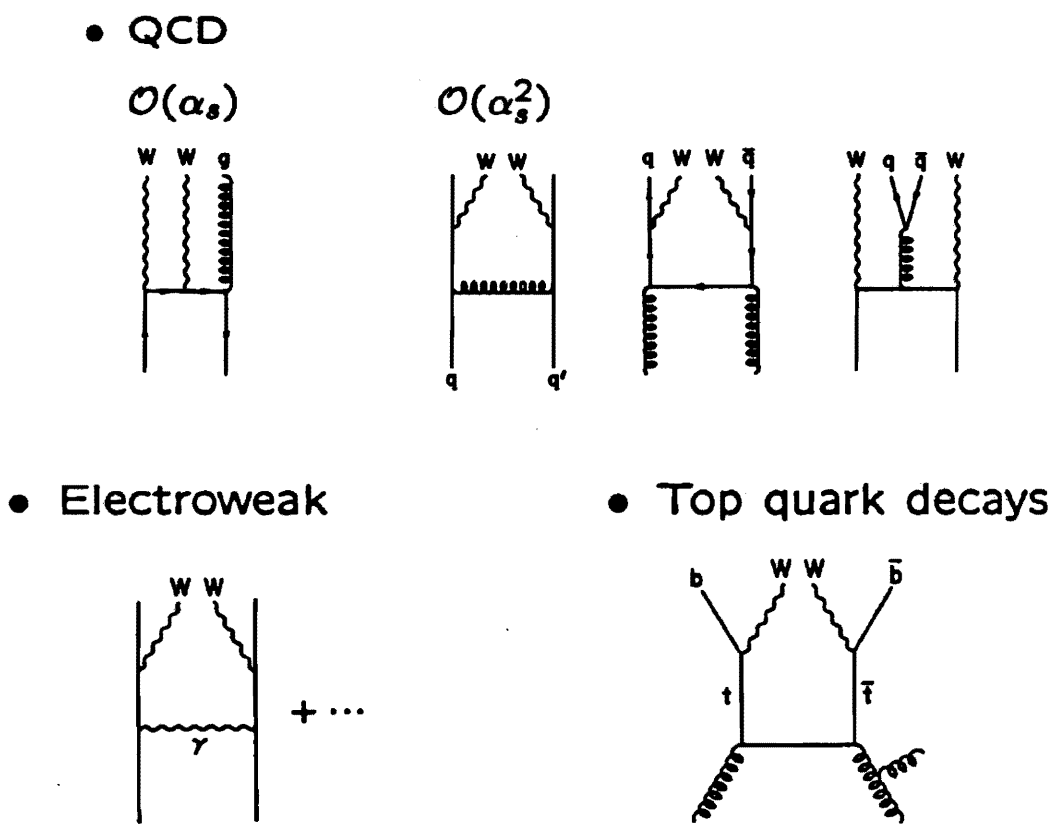


Fig. 3. Representative backgrounds to $qq \to qqW^+W^-$ with single forward jet tagging.

An optimized choice of the single forward jet tag for SSC energies is[6,16]

$$3 < |\eta_j(\text{tag})| < 5 \,, \tag{10a}$$

$$E_j(\text{tag}) > 3\,\text{TeV} \,, \tag{10b}$$

which retains about 25% of the $m_H = 1\,\text{TeV}$ signal, essentially eliminates the QCD background, and reduces the $t\bar{t}j$ background by a factor of 100 to the level of the signal. In the $\eta_j(\text{tag})$, $E_j(\text{tag})$ lego plot of Fig 4 one can see the effectiveness of the above criteria in suppressing the backgrounds relative to the signal.

The central jet veto is needed to further reduce the contributions from $t\bar{t}$ events, which give high $p_T$ $b$-jets in the central region from the $t$-decay. If events with jets having

$$|\eta_j| < 3 \,, \qquad p_{Tj} > 60\,\text{GeV} \tag{11}$$

are vetoed, the $t\bar{t}j$ background is further reduced by a factor of 10, while retaining $\sim 70\%$ of the remaining $m_H = 1\,\text{TeV}$ signal (an overall signal efficiency of 20%).

The energy distribution of the tag-jet after the central jet veto is shown in Fig. 5, relaxing the previous $E_j(\text{tag}) > 3\,\text{TeV}$ requirement. The Higgs boson signal appears as a distinct break in the tag-jet energy distribution which is a dramatic flag for discovery. The mass $m_H$ can be reasonably well estimated from the $\ell^+\ell^-$ invariant mass

distribution (peaking near $\frac{1}{2}m_H$) or the $\ell^+\ell^-$, $\not{p}_T$ cluster transverse mass (peaking near $\frac{3}{4}m_H$). Because the Higgs peak is so broad, the lack of full reconstruction of $m_H$ in $\ell\nu\ell\nu$ events is not a problem.

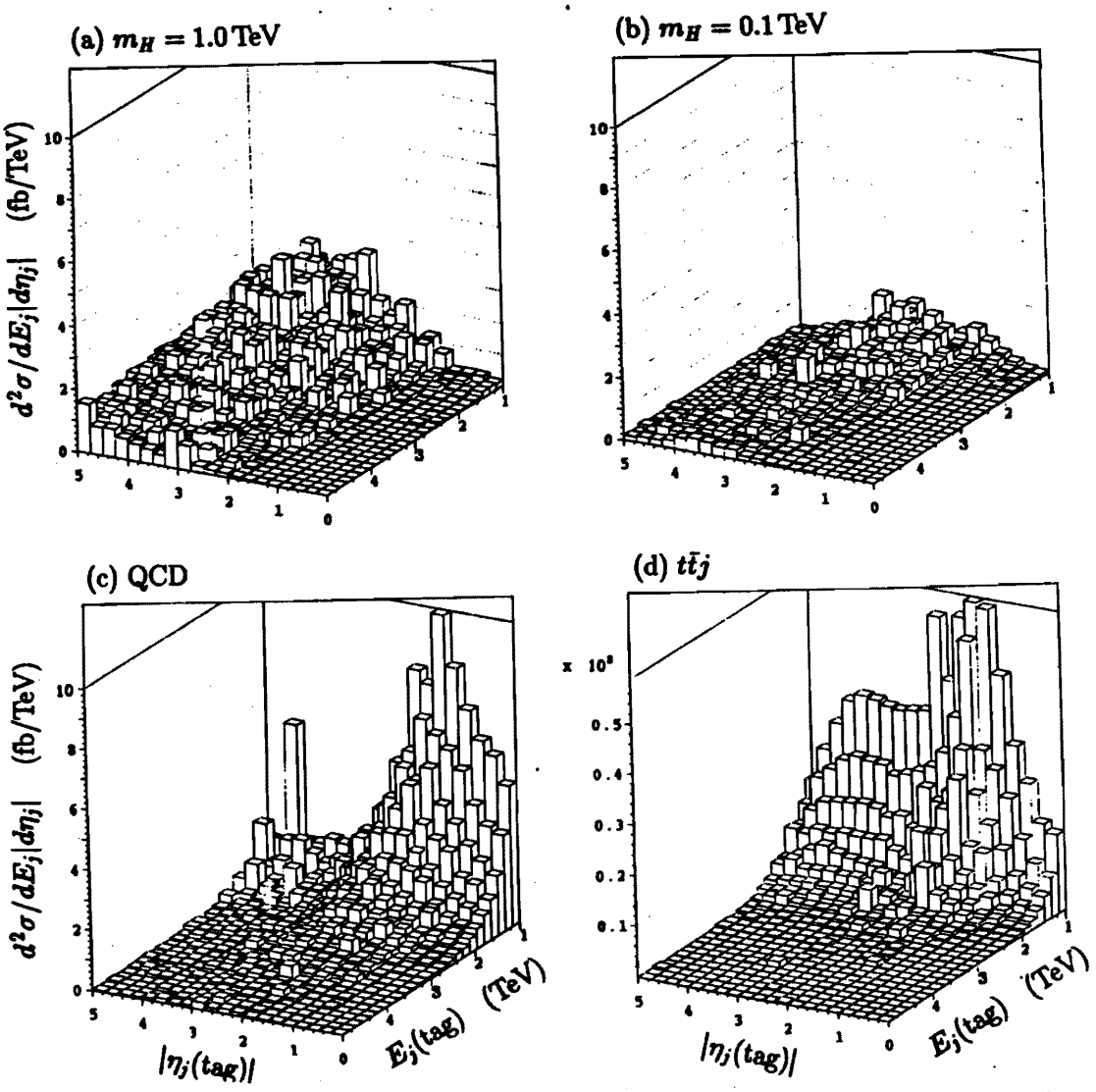


Fig. 4. Lego plot of tagged jet energy and pseudorapidity for weak boson scattering events and the $WWj$ and $t\bar{t}j$ backgrounds at the SSC. Note the different scale for the $t\bar{t}j$ background. From Ref. 16.

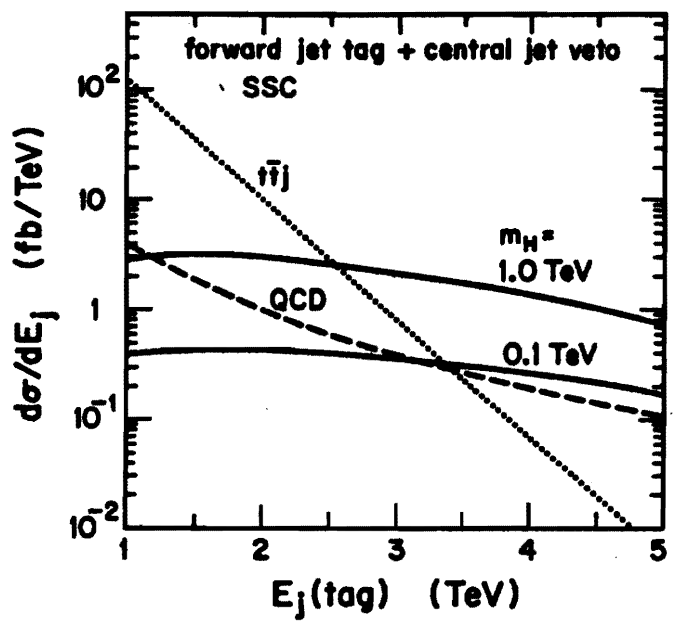


Fig. 5. Energy distribution of the tagged jet ($3 < |\eta_j| < 5$) at SSC energies after the central jet veto (rejection of events with jets having $|\eta_j > 3|$ and $p_{Tj} > 60\,\text{GeV}$). From Ref. 16.

The bottom line event rates for signal and background after cuts are summarized in Table 1. At the SSC the significance of a 1 TeV Higgs boson is $S/\sqrt{B} \approx 8$.

Table 1. Higgs boson signal and background events in the $WW \to \ell\nu\ell\nu$ channel after acceptance cuts for SSC luminosity of $10\,\text{fb}^{-1}$. From Ref. 16.

| | $WW$ signal $m_H$ (TeV) = 1 | 0.6 | 0.1 | QCD | $t\bar{t}j$ $m_t = 140\,\text{GeV}$ (100) | |
|---|---|---|---|---|---|---|
| SSC ($E_j > 3\,\text{TeV}$) | 46 | 46 | 10 | 6 | 4.2 | (16) |
| LHC ($E_j > 2\,\text{TeV}$) | 4.6 | 5.3 | 0.9 | 0.8 | 0.45 | (1.8) |

Forward jet tagging is also very valuable in other channels. In "$H$" $\to ZZ \to 4\ell$ the $gg$ and $WW$ fusion contributions can be separated so that both $t\bar{t}H$ and $WWH\,(ZZH)$ couplings can be determined. In extracting the contributions of $WW$ ($ZZ$) fusion, the jet tag reduces the $q\bar{q} \to ZZ$ continuum background.[6] In $WZ$ production jet tagging is essential to suppress the $q\bar{q}' \to WZ$ background.[21]

In conclusion, it is a necessity that SSC/LHC detectors have the capability to tag forward jets in order to study the physics of electroweak symmetry breaking in the $WW$ sector.

## 3. Detectability of the Minimal Supersymmetric Standard Model (MSSM) Higgs Bosons

Two fundamental theoretical issues would be settled by the discovery of MSSM Higgs bosons: electroweak symmetry breaking is a Higgs phenomenon and supersymmetry is the solution to the gauge hierarchy problem. The Higgs sector of the MSSM model has five spin-zero particles;[22] two CP-even neutral bosons $h$ and $H$ (with $m_h < m_H$), a CP-odd neutral boson $A$ and two charged bosons $H^{\pm}$. At tree level the masses and couplings are specified by two parameters $m_A$ and $\tan\beta = v_2/v_1$. A mixing angle $\alpha$ that appears in the $h$ and $H$ couplings is also determined by these two parameters. The couplings are summarized in Table 2.

Table 2: Couplings of MSSM Higgs Bosons

| | $t\bar{t}$ | $b\bar{b}$, $\tau^+\tau^-$ | $WW$, $ZZ$ |
|---|---|---|---|
| $h$ | $\frac{\cos\alpha}{\sin\beta}$ | $-\frac{\sin\alpha}{\cos\beta}$ | $\sin(\beta-\alpha)$ |
| $H$ | $\frac{\sin\alpha}{\sin\beta}$ | $\frac{\cos\alpha}{\cos\beta}$ | $\cos(\beta-\alpha)$ |
| $A$ | $\frac{\cos\beta}{\sin\beta}$ | $\frac{\sin\beta}{\cos\beta}$ | 0 |

Yukawas:

$$\lambda_t = \frac{m_t}{v_2} = \frac{m_t}{v\sin\beta}$$

$$\lambda_b = \frac{m_b}{v_1} = \frac{m_b}{v\cos\beta}$$

The $H$ and $h$ boson share couplings to gauge bosons and to quarks. The $A$ boson does not couple to gauge bosons. At large $\tan\beta$ couplings to $b$ and $\tau$ are enhanced.

At tree level $m_h < M_Z$ and $m_H > M_Z$. However it is now known that the Higgs boson masses and the mixing angle $\alpha$ may be appreciably modified by radiative corrections.[23] In the approximation of a single SUSY mass scale $\tilde{m}$, radiative corrections give

$$\begin{matrix} m_h < \\ m_H > \end{matrix} \sqrt{M_Z^2 + \epsilon}\,, \tag{12}$$

where the radiative effects are approximately given by

$$\epsilon \simeq \frac{3g^2}{8\pi M_W^2} m_t^4 \ln\left(1 + \frac{\tilde{m}^2}{m_t^2}\right) . \tag{13}$$

For $\tilde{m} = 1\,\text{TeV}$ and $m_t = 150\,\text{GeV}$ ($200\,\text{GeV}$), the extreme possibilities for the $h$, $H$ masses are $m_h \lesssim 116\,\text{GeV}$ ($140\,\text{GeV}$) $\lesssim m_H$. Figure 6 shows contours of $m_h$, $m_H$ and $m_{H^\pm}$ in the ($m_A$, $\tan\beta$) plane, over reasonable ranges of the $m_A$, $\tan\beta$ parameters, taking into account representative contributions from soft-supersymmetry breaking parameters.[24,25] The effect of the radiative corrections is to increase $|\alpha|$ as illustrated[24] in Fig. 7. The corresponding directions in the changes of the couplings are as follows:

Table 3: Directions of change in Higgs boson couplings due to radiative corrections.

| | $t\bar{t}$ | $b\bar{b}$, $\tau^+\tau-$ | $WW$, $ZZ$ |
|---|---|---|---|
| $h$ | $\downarrow$ | $\uparrow$ | $\downarrow^*$ |
| $H$ | $\uparrow$ | $\downarrow$ | $\uparrow^*$ |

*for $\tan\beta > 1$

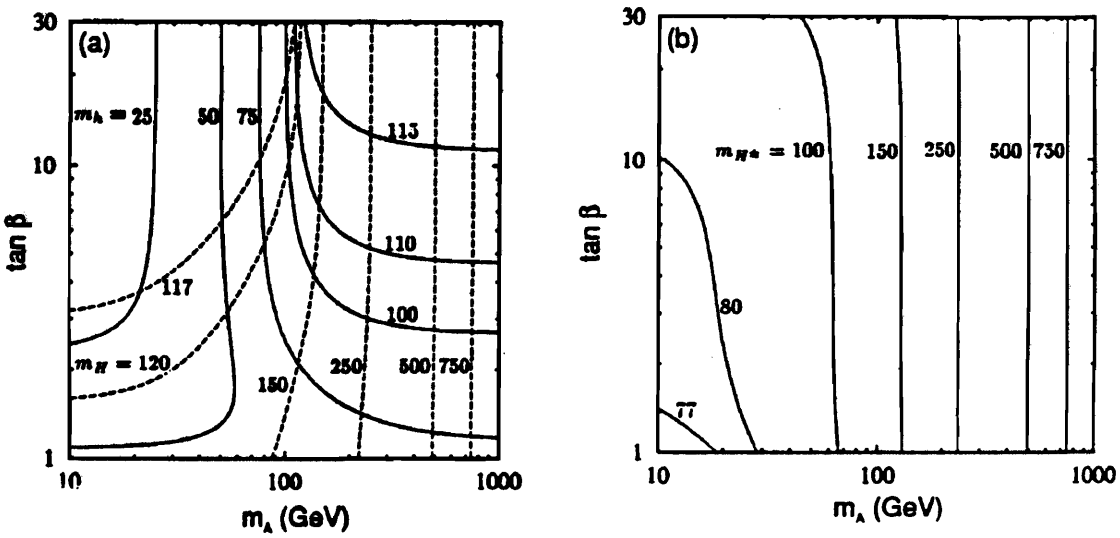


Fig. 6. Contour plots of MSSM Higgs boson masses in the ($m_A$, $\tan\beta$) plane for $m_t = 150\,\text{GeV}$ and SUSY mass scale of 1 TeV. From Ref. 25.

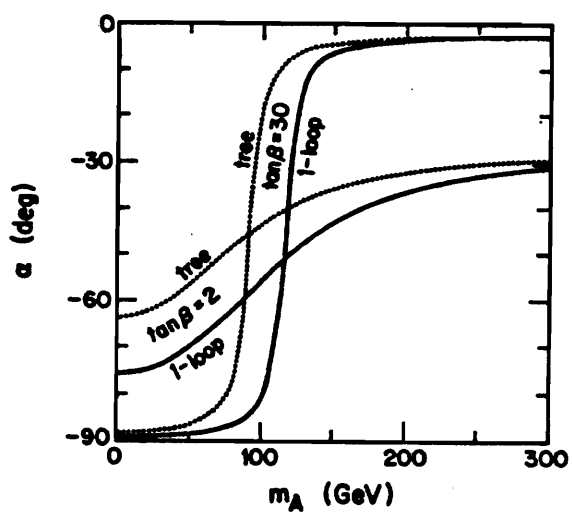


Fig. 7. The mixing angle $\alpha$ in the CP-even Higgs boson sector versus $m_A$ for $\tan\beta = 2$ and 30, with $m_t = 150\,\text{GeV}$ and $\tilde{m} = 1\,\text{TeV}$. From Ref. 24.

The implication of these radiative corrections for MSSM Higgs boson search at $e^+e^-$ and $pp$ colliders have recently been addressed.[24–30] The results of the various analyses are qualitatively similar; conclusions from Refs. 24,25 are summarized here.

At LEP I searches for the processes $e^+e^- \to Z \to Z^*h$, $Ah$ have excluded most of the region with $m_A \lesssim 50\,\text{GeV}$. The domain ruled out by ALEPH[31] is shown in Fig. 8(a),(b). The excluded regions are sensitive to the value of $m_t$ due to the $m_t$-dependence of $m_h$ and the mixing angle $\alpha$.

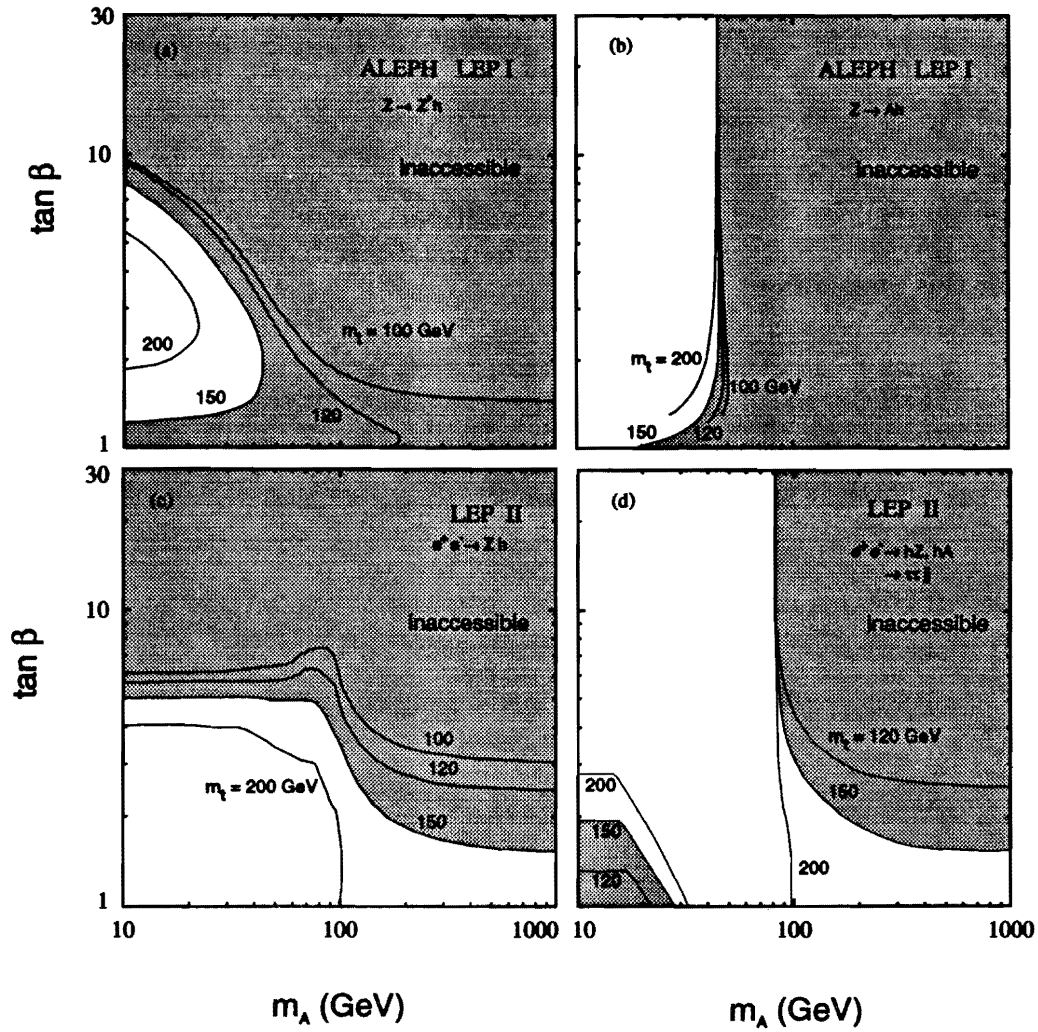


Fig. 8. Excluded regions of the ($m_A$, $\tan\beta$) plane from the ALEPH experiment at LEP I and limits of detectability of MSSM Higgs bosons at LEP II, including electroweak radiative corrections. From Ref. 25.

At LEP II the coverage is increased to $m_A \lesssim 100\,\text{GeV}$ for any $\tan\beta$, as shown in Fig. 8(c),(d). This coverage assumes CM energy $\sqrt{s} = 200\,\text{GeV}$ and luminosity $\mathcal{L} = 0.5\,\text{fb}^{-1}$.[32] The $e^+e^- \to Zh$ results are inferred by a rescaling of an earlier $e^+e^- \to ZH_{\text{SM}}$ simulation[33] indicating that $m_{H_{\text{SM}}} \lesssim 80\,\text{GeV}$ could be discovered. The $e^+e^- \to hZ$, $hA \to \tau\tau jj$ results[25] are obtained by rescaling a simulation by Janot[30] at $\sqrt{s} = 500\,\text{GeV}$ to the LEP II $\sqrt{s}$ and $\mathcal{L}$ (the major background is $e^+e^- \to ZZ$). Our criteria for discovery is 1 Higgs boson peak with $S/\sqrt{B} > 4$ ($S > 4$ counts) in a 10 GeV mass bin at Higgs resonance peaks ($S$ = signal, $B$ = background). However if $h$, $A$ are under the $Z$ peak ($\pm 5\,\text{GeV}$), $S/\sqrt{B} > 6$ is imposed for discovery since we must rely on normalization ($S$ = Higgs peak + $Z$ peak from $Zh$, $B = Z$ peak from $ZZ$).

At the SSC or LHC $pp$ machines, analyses of MSSM Higgs boson detectability are complicated by SM background considerations.[34] For definiteness the present discussion

focuses on the Higgs discovery potential of the SDC and GEM detectors at the SSC with $\sqrt{s} = 40\,\text{TeV}$ and $\mathcal{L} = 20\,\text{fb}^{-1}$, but similar results are obtainable at the LHC if the luminosity is an order of magnitude higher. For discovery, one Higgs boson peak with $S/\sqrt{B} > 4$ is usually assumed here. A value $m_t = 150\,\text{GeV}$ for the top-quark mass is addressed here; similar conclusions are reached for other $m_t$ values (see Ref. 25).

Detection of the inclusive $gg \to$ Higgs boson $\to \gamma\gamma$ signals over the large SM backgrounds requires excellent $\gamma\gamma$ mass resolution, $\Delta m/m(\gamma\gamma) \lesssim 1\%$, achievable with the GEM LAr detector.[35] Figure 9(a) shows the accessible region of the $(m_A, \tan\beta)$ plane for this final state.

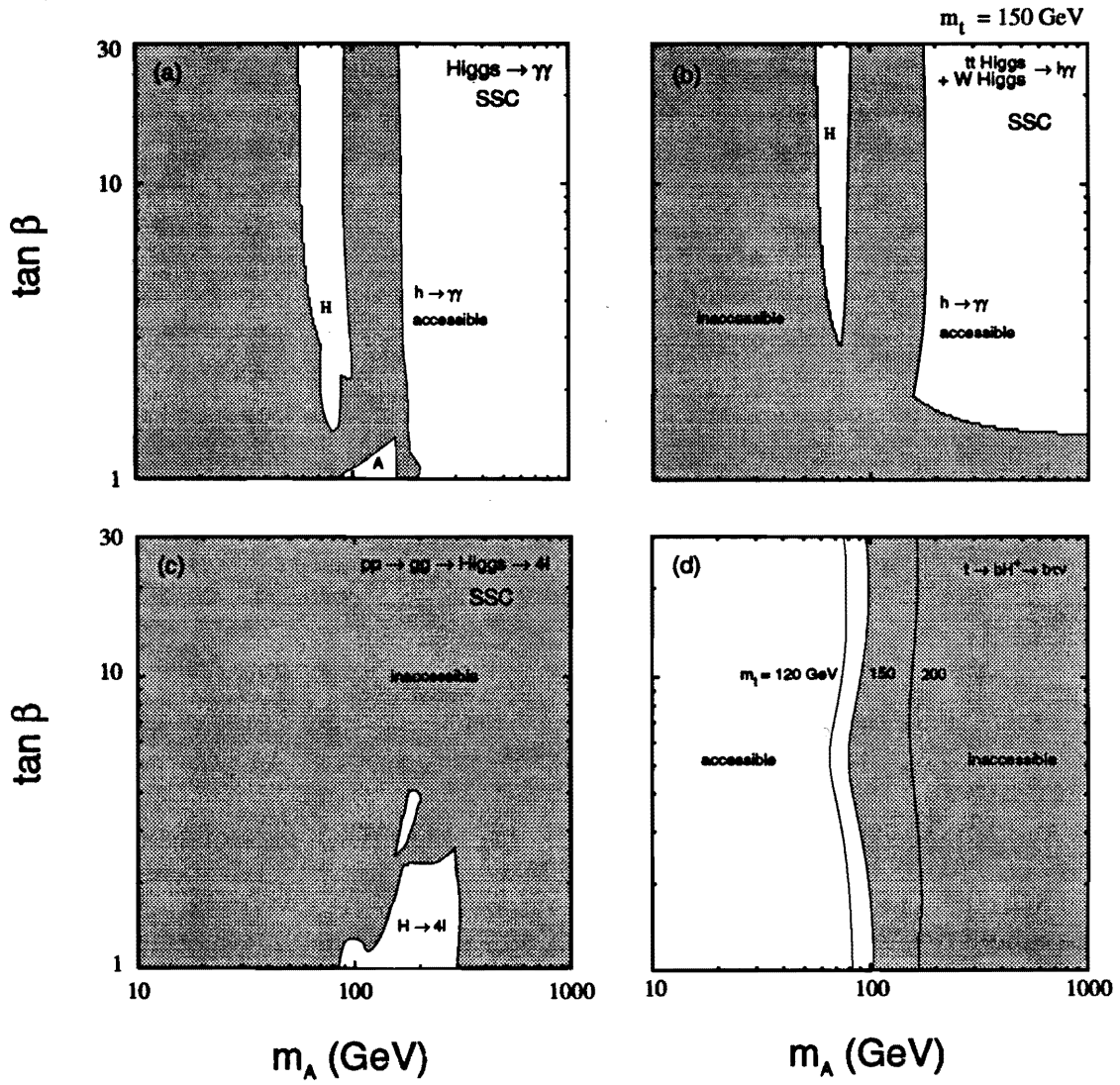


Fig. 9. Potential for discovery of MSSM Higgs bosons at the SSC via a) untagged $\gamma\gamma$, b) lepton tagged $\gamma\gamma$, c) four-lepton and d) $t \to bH^+$, $H^+ \to \tau^+\nu$, $\tau^+ \to \pi^+\nu$ signals. From Ref. 25.

With a lepton tag from $W$-boson decay in $t\bar{t}$ Higgs or $W$ Higgs production, the $\gamma\gamma$

signal can be identified in the SDC detector[36] with a mass resolution $\Delta m(\gamma\gamma) \lesssim 3\,\mathrm{GeV}$. Figure 9(b) shows the corresponding accessible region of the MSSM parameter space.

The "gold-plated" $H \to ZZ \to 4\ell$ decay mode provides $S > 10$ events in the region shown in Fig. 9(c); the failure of the gold-plated signature over large regions of the parameter space is due to smaller $HWW$ and $HZZ$ branching fractions compared to the SM values, because of reduced couplings and competing modes.

The decay of the top quark to a charged Higgs boson, $t \to bH^+ \to b\tau^+\nu_\tau \to b(\pi^+\bar{\nu}_\tau)\nu_\tau$ can be identified as violations in lepton universality expected from $W$ decays.[35–37] A $S/\sqrt{B} > 5$ signal of this sort probes charged Higgs boson masses within about 20 GeV of $m_t$, as illustrated in Fig. 9(d).

The preceding accessible regions for MSSM Higgs boson discovery at the SSC are combined in Fig. 10. Although many parameter regions are covered by more than one reaction, there remains an inaccessible window for $m_A$ between 90 and 170 GeV. A blown-up view of this inaccessible region is presented in Fig. 11, along with the corresponding $m_h$ and $m_H$ masses that are not ruled out.

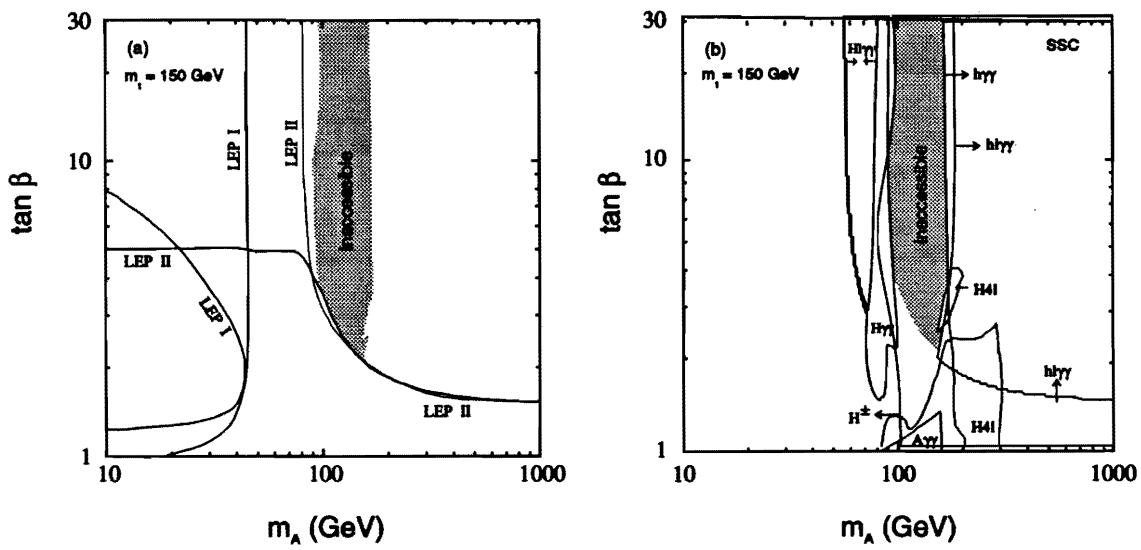


Fig. 10. Combined accessible discovery regions for at least one MSSM Higgs boson at a) LEP and b) SSC. From Ref. 25.

How many MSSM Higgs bosons can be seen in LEP and SSC experiments? This question is answered in Fig. 12. For $m_A \lesssim 100\,\mathrm{GeV}$, there are many possibilities for observing 1, 2, 3 or 5 of the MSSM Higgs bosons. For $m_A$ large only $h$ is likely to be discovered, since in this region the couplings of $h$ approach those of $H_{\mathrm{SM}}$ and the couplings of the other Higgs bosons are suppressed.

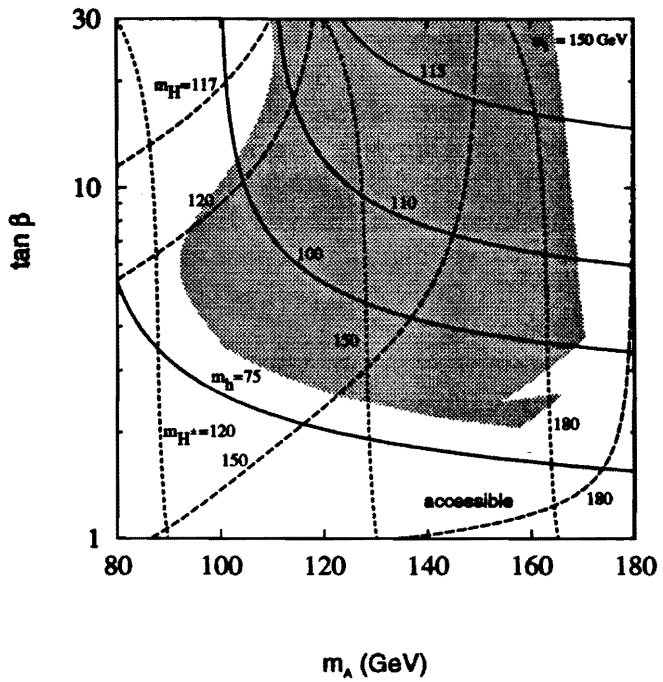


Fig. 11. Expanded view of the inaccessible region from Fig. 10 with contours of the $m_h$, $m_H$ and $m_{H^\pm}$ masses. From Ref. 25.

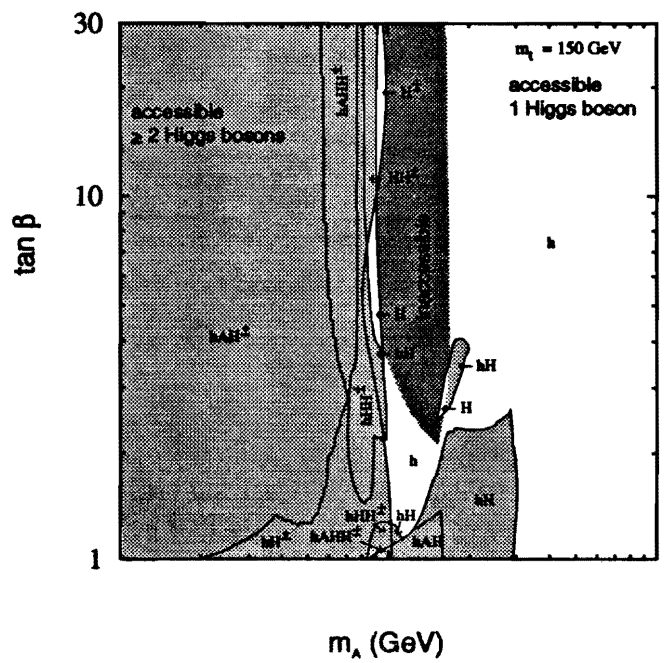


Fig. 12. Discovery regions for more than one MSSM Higgs boson, for $m_t = 150\,\mathrm{GeV}$ and $\tilde{m} = 1\,\mathrm{TeV}$. From Ref. 25.

## 4. What $e^+e^-$ could make a "no-lose" search for MSSM Higgs boson?

In order to definitively test the MSSM model, complete coverage of the parameter space $10 < m_A < 1000\,\text{GeV}$, $1 < \tan\beta < 30$ and $100 < m_t < 200\,\text{GeV}$ is a desirable goal. It is therefore appropriate to consider what future $e^+e^-$ collider could provide this coverage, since there remains a region that is inaccessible to LEP II and SSC/LHC. The conclusions of the study presented in Ref. 38 will be summarized here. The largest contributions to Higgs boson production at $e^+e^-$ collisions at lower energies are

$$e^+e^- \to Zh,\ Ah,\ AH,\ AH \tag{14}$$

as shown[39] in Fig. 13. In the $m_A \to \infty$ limit,

$$m_h \to \sqrt{M_Z^2 + \epsilon}\,; \qquad m_H,\, m_{H^+} \to m_A\,. \tag{15}$$

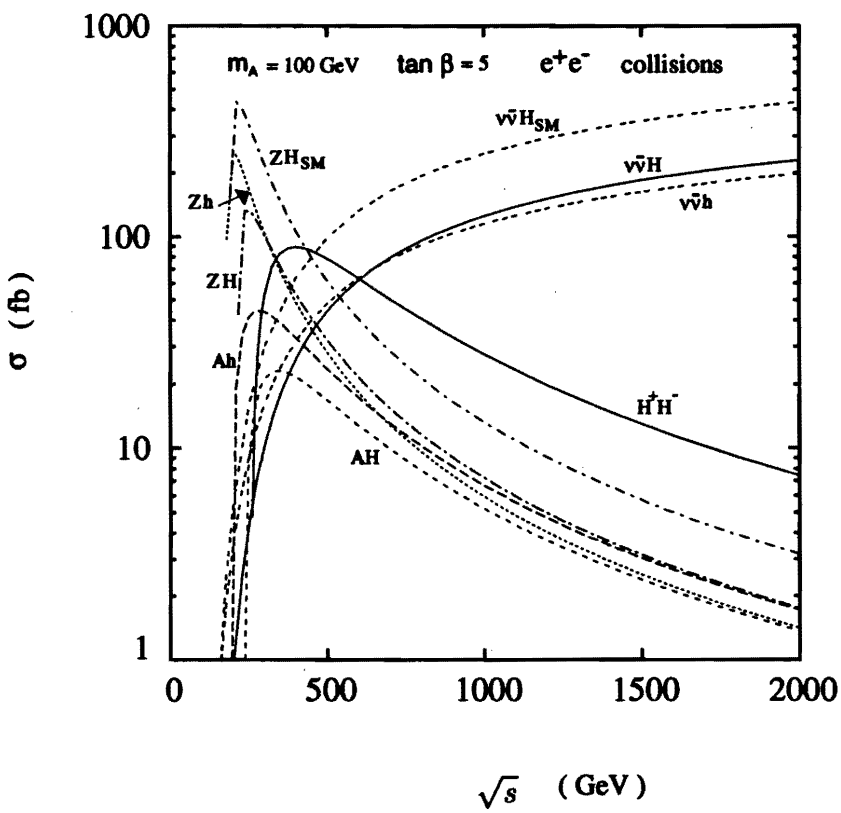


Fig. 13. Cross sections versus CM energy for MSSM Higgs boson production at $e^+e^-$ colliders. From Ref. 39.

Hence $e^+e^- \to Zh$ is essential to the Higgs boson search and $e^+e^- \to Ah$ is also necessary to cover regions where the $ZZh$ coupling is suppressed. In the following we consider searches based on

$$e^+e^- \to Zh,\ Ah,\ ZH,\ AH \to \tau\tau jj\,, \tag{16}$$

for which the dominant background is

$$e^+e^- \to ZZ \to \tau\tau jj \,. \tag{17}$$

This approach is conservative since $Zh$ production with $Z \to \nu\bar{\nu}$, $\ell\bar{\ell}$ decays will also help.

The principal factors that determine the Higgs boson discovery regions are (1) the CM energy $\sqrt{s}$, (2) the luminosity $\mathcal{L}$, and (3) the top mass $m_t$. To be able to achieve full coverage of the ($m_A$, $\tan\beta$) space, the CM energy must exceed the $Zh$ threshold energy for the maximum $m_h$ mass. At $m_t = 150\,\text{GeV}$, this threshold is

$$m_h\,(\text{max}) + M_Z = 207\,\text{GeV} \,. \tag{18}$$

The coverage that can be obtained with $\mathcal{L} = 1\,\text{fb}^{-1}$ and $10\,\text{fb}^{-1}$ is shown in Fig. 14(a) and 14(b). At $\sqrt{s} = 215\,\text{GeV}$ (230 GeV) a luminosity of $\mathcal{L} = 20\,\text{fb}^{-1}$ ($10\,\text{fb}^{-1}$) gives full coverage. At $m_t = 200\,\text{GeV}$, the threshold is

$$m_h\,(\text{max}) + M_Z = 240\,\text{GeV} \,. \tag{19}$$

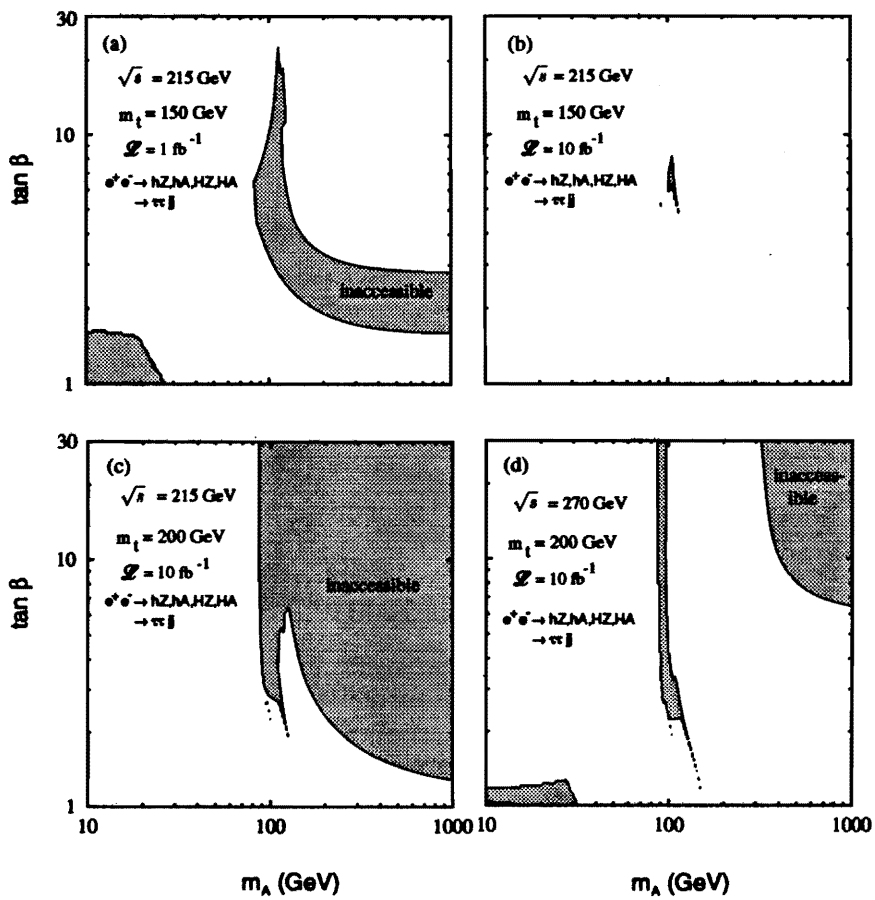


Fig. 14. Discovery regions for MSSM Higgs bosons in the ($m_A$, $\tan\beta$) plane from the $e^+e^- \to Zh$, $Ah$, $ZH$, $AH \to \tau\tau jj$ signals, CM energies and luminosities. From Ref. 38.

At $\sqrt{s} = 270\,\mathrm{GeV}$, $\mathcal{L} = 20\,\mathrm{fb}^{-1}$ provides full coverage. Figure 15 summarizes the combinations of $e^+e^-$ collider parameters $\sqrt{s}$ and $\mathcal{L}$ that would achieve complete coverage of the $(m_A, \tan\beta)$ plane for several choices of $m_t$. The "no-lose" discovery regions lie above the limiting curves in this figure. If the top quark is found in experiments at the Fermilab Tevatron, we will then know the design parameters of an $e^+e^-$ collider that can settle this crucial issue.

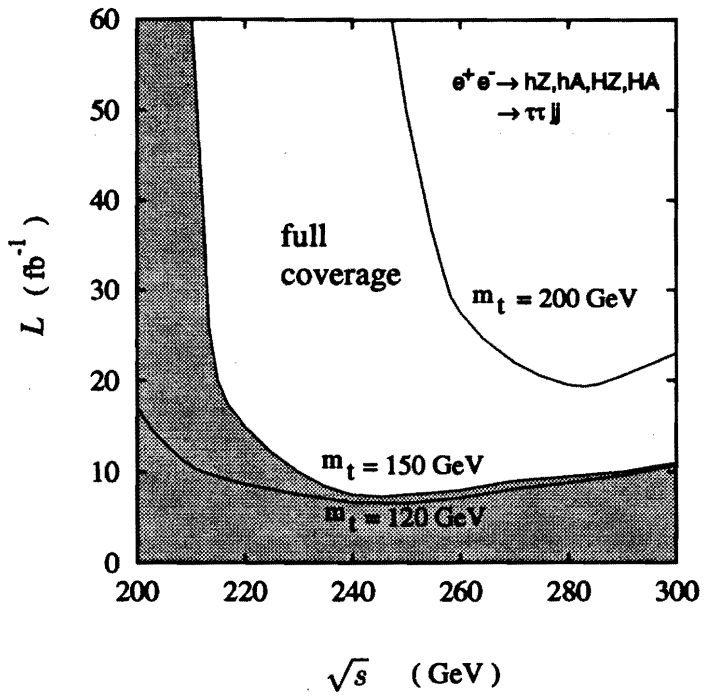


Fig. 15. Combinations of $e^+e^-$ collider energies $\sqrt{s}$ and integrated luminosities $\mathcal{L}$ that would yield complete coverage for MSSM Higgs bosons throughout the $(m_A, \tan\beta)$ regions of interest. From Ref. 38.

## Acknowledgments

The contributions of my collaborators Micheal Berger, Kingman Cheung, Tao Han, Roger Phillips, Alan Stange and Dieter Zeppenfeld to the work discussed in this report is gratefully acknowledged. Special thanks are due to Roger Phillips and Alan Stange for helpful discussions in the preparation of this report. This report was written at the Aspen Center for Physics. This work was supported in part by the U.S. Department of Energy under contract No. DE-AC02-76ER00881, in part by the Texas National Research Laboratory Commission under grant No. RGFY9173, and in part by the University of Wisconsin Research Committee with funds granted by the Wisconsin Alumni Research Foundation.

## References


1. V. Barger, A. L. Stange and R. J. N. Phillips, *Phys. Rev.* **D45** (1992) 1484.
2. R. W. Brown and K. O. Mikaelian, *Phys. Rev.* **D19** (1979) 922; E. Eichten, I. Hincliffe, K. Lane and C. Quigg, *Rev. Mod. Phys.* **56** (1984) 579.
3. See e.g. K. Hagiwara et al., *Nucl. Phys.* **B282** (1987) 253; D. Zeppenfeld and S. Willenbrock, *Phys. Rev.* **D37** (1988) 175; U. Baur and D. Zeppenfeld, *Nucl. Phys.* **B308** (1988) 127; G. L. Kane, J. Vidal and C.-P. Yuan, *ibid.* **D39** (1988) 2617.
4. D. A. Dicus, C. Kao and W. W. Repko, *Phys. Rev.* **D36** (1987) 1570; E. W. N. Glover and J. J. van der Bij, *Nucl. Phys.* **B321** (1989) 561.
5. U. Baur and E. W. N. Glover, *Phys. Rev.* **D44** (1991) 99.
6. V. Barger, Kingman Cheung, T. Han, J. Ohnemus and D. Zeppenfeld, *Phys. Rev.* **D44** (1991) 1426.
7. M. Golden and S. R. Sharpe, *Nucl. Phys.* **B261** (1985) 217; V. Barger and T. Han, *Phys. Lett.* **B212** (1988) 117.
8. V. Barger, T. Han and H. Pi, *Phys. Rev.* **D41** (1990) 824.
9. V. Barger, A. L. Stange and R. J. N. Phillips, *Phys. Rev.* **D44** (1991) 1987; *Phys. Rev.* **D45** (1992) 1751.
10. Z. Kunszt, *Nucl. Phys.* **247** (1984) 339; Z. Kunszt and W. J. Stirling, *Phys. Lett.* **B171** (1986) 307; J. F. Gunion and Z. Kunszt, *Phys. Lett.* **159B** (1985) 167; *Phys. Lett.* **B176** (1986) 477.
11. H. Baer, X. Tata, and J. Woodside, *Phys. Rev.* **D41** (1990) 906; **D42** (1991) 1568; also see H. Baer, V. Barger, D. Karatas and X. Tata, *Phys. Rev.* **D36** (1987) 961; M. Barnett, J. Gunion and H. Haber, *Phys. Rev.* **D37** (1988) 1892.
12. M. S. Chanowitz and M. Golden, *Phys. Rev. Lett.* **61** (1988) 1053; **63** (1989) 466(E); M. S. Chanowitz and M. K. Gaillard, *Nucl. Phys.* **B261** (1985) 375; M. S. Chanowitz, *Ann. Rev. Nucl. Part. Sci.* **38** (1985) 323; **63** (1989) 466(E); A. Dobado and M. J. Herrero, *Phys. Lett.* **B288** (1989) 195; G. Kane and C. Yuan, *Phys. Rev.* **D40** (1989) 2231; F. Donoghue and C. Ramirez, *Phys. Lett.* **B234** (1990) 361; A. Dobado, M. J. Herrero and T. N. Trong, *ibid.* B235 (1990) 129; D. Dicus and W. Repko, *Phys. Rev.* **D42** (1990) 3660; V. Barger, K. Cheung, T. Han and R. J. N. Phillips, *Phys. Rev.* **D42** (1990) 3052; M. S. Berger and M. S. Chanowitz, *Phys. Lett.* **B267** (1991) 416; LBL-31343 (1991); D. Dicus, J. F. Gunion and R. Vega, *ibid.* **B258** (1991) 475; M. Veltman, talk at the *SSC Symposium*, Madison, Wisconsin (1992).
13. R. N. Cahn et al, *Phys. Rev.* **D35** (1987) 1626; V. Barger, T. Han and R. J. N. Phillips, *ibid.* **D37** (1988) 2005.
14. R. Kleiss and W. J. Stirling, *Phys. Lett.* **B200** (1988) 193; D. Froideveaux, CERN Report.
15. Yu. L. Dokshitzer, V. A. Khoze and S. I. Troyan in *Proc. 6th Int. Conf. on Physics in Collision* (1986) ed. by M. Derrick (World Scientific, Singapore, 1987), p. 417.
16. V. Barger, Kingman Cheung, T. Han and D. Zeppenfeld, *Phys. Rev.* **D44** (1991) 2701.
17. D. A. Dicus, J. F. Gunion and R. Vega, *Phys. Lett.* **B258** (1991) 475.
18. Yu. L. Dokshitzer, V. A. Khoze and T. Sjörstrand, *Phys. Lett.* **B274** (1992) 116.
19. J. D. Bjorken, *Int. J. Mod. Phys.* **A7** (1992) 4189.

20. H. Chehime et al., Univ. of Wisconsin report MAD/PH/700 (1992); R. S. Fletcher and T. Stelzer, Univ. of Wisconsin report MAD/PH/710 (1992).
21. V. Barger, Kingman Cheung, T. Han, A. L. Stange and D. Zeppenfeld, Univ. of Wisconsin-Madison report MAD/PH/684 (1991), *Phys. Rev. D* (in press).
22. See e.g. J. Gunion, H. Haber, G. Kane and S. Dawson, *The Higgs Hunter's Guide*, Addison-Wesley (1990).
23. S. P. Li and M. Sher, *Phys. Lett.* **B140** (1984) 339; J. F. Gunion and A. Turski, *Phys. Rev.* **D39** (1989) 2701; **D40** (1989) 2325, 2333; M. S. Berger, *Phys. Rev.* **D41** (1990) 225; Y. Okada et al., *Prog. Theor. Phys.* **85** (1991) 1; *Phys. Lett.* **B262** (1991) 54; H. Haber and R. Hempfling, *Phys. Rev. Lett.* **66** (1991) 1815; J. Ellis et al., *Phys. Lett.* **B257** (1991) 83; R. Barbieri et al., *Phys. Lett.* **B258** (1991) 167; J. Lopez and D. V. Nanopoulos, *Phys. Lett.* **B266** (1991) 397; A. Yamada, *Phys. Lett.* **B263** (1991) 233; M. Drees and M. N. Nojiri, KEK-TH-305 (1991); R. Hempfling, SCIPP-91/39 (1991); D. M. Pierce, A. Papadopoulos and S. Johnson, *Phys. Rev. Lett.* **68**, 3678 (1992); M. A. Diaz and H. E. Haber, *Phys. Rev.* **D45** (1992) 4246; H. E. Haber and R. Hempfling, SCIPP-91-33 (1992).
24. V. Barger, M. S. Berger, A. L. Stange and R. J. N. Phillips, *Phys. Rev.* **D45** (1992) 4128.
25. V. Barger, Kingman Cheung, R. J. N. Phillips and A. L. Stange, Univ. of Wisconsin-Madison report MAD/PH/696 (1992).
26. J. Ellis, G. Ridolphi and F. Zwirner, *Phys. Lett.* **B262**, 477 (1991); A. Brignole et al., *Phys. Lett.* **B271** (1991) 123; R. Barbieri and M. Frigeni, *Phys. Lett.* **B258** (1991) 395; J. Kalinkowski, Munich report TUM-T31-14/91.
27. H. Baer, M. Bisset, C. Kao and X. Tata, Florida State Univ. report FSU-HEP-911104 (1991); H. Baer, C. Kao, X. Tata and D. Dicus, FSU-HEP-920724 (1992).
28. Z. Kunszt and F. Zwirner, in *Proceedings of the Large Hadron Collider Workshop at Aachen*, CERN 90-10; revised results in CERN-TH.6150/91; F. Zwirner, report to this meeting.
29. J. F. Gunion, R. Bork, H. E. Haber and A. Seiden, U. C. Davis report UCD-91-29; J. F. Gunion and L. H. Orr, report UCD-91-15; J. F. Gunion, H. E. Haber, and C. Kao, UCD-91-32; J. F. Gunion, UCD-92-20 (1992), to appear in *Perspectives in Higgs*, ed. by G. Kane, World Scientific.
30. P. Janot, Orsay preprints LAL 91-61, talk presented at the *ICFA Workshop*, Saariselka, Finland (1991), and LAL 92-27, talk presented at the *27th Recontres de Moriond: Electroweak Interactions and Unified Theories*, Les Arcs, France (1992); J.-F. Grivaz, Orsay preprint LAL 91-63 (1991).
31. ALEPH Collaboration, D. Decamp et al., *Phys. Lett.* **B246** (1990) 306; **B265** (1991) 475, and CERN-PPE/91-149 to be published in Physics Reports; DELPHI Collaboration: P. Abreu et al., *Phys. Lett.* **B245** (1990) 276; *Nucl. Phys.* **B373** (1992) 3; L3 Collaboration: B. Adeva et al., *Phys. Lett.* **B251** (1990) 311; **B283** (1992) 454. OPAL Collaboration: M. Z. Akrawy et al., *Z. Phys.* **C49** (1991) 1.
32. C. Rubbia, in *Proc. LEP-HEP 91*, ed. by S. Hegarty et al., World Scientific (1991) p. 439.
33. S. L. Wu et al., ECFA Workshop on LEP 200, CERN 87-08, p. 312.

34. See *Proceedings of 1990 Snowmass Summer Study on High Energy Physics*; *Proceedings of Large Hadron Collider Workshop at Aachen 1990*, CERN 90-10.
35. GEM Letter of Intent, contact persons B. Barish, W. Willis: GEM TN-92-49.
36. Solenoidal Detector Collaboration, Expression of Interest, spokesperson G. H. Trilling, SSC-EOI0003 (1990) and SDC Technical Design Report SDC-92-201 (April 1992).
37. V. Barger and R. J. N. Phillips, *Phys. Lett.* **B201** (1988) 553; *Phys. Rev.* **D41** (1990) 894; V. Barger, J. L. Hewett and R. J. N. Phillips, *Phys. Rev.* **D41** (1990) 3421; R. M. Godbole and D. P. Roy, *Phys. Rev.* **D43** (1991) 3640; M. Drees and D. P. Roy, *Phys. Lett.* **B269** (1991) 155; D. P. Roy, *Phys. Lett.* **B283**, 403 (1992).
38. V. Barger, Kingman Cheung, R. J. N. Phillips and A. L. Stange, Univ. of Wisconsin-Madison report MAD/PH/704 (1992).
39. V. Barger, Kingman Cheung, R. J. N. Phillips and A. L. Stange, Univ. of Wisconsin-Madison report MAD/PH/705 (1992).

RETURN TO FERMI LIBRARY
ROUTE TO
NAME
LOCATION
OZELIS
346
Denisov
352
HOTVAT
220